OPTIMIZATION OF INTEGRATED THERMOELECTRIC/MICROCOMBUSTOR DEVICES

K. Bijjula[1], E. D. Wetzel[2] and D. G. Vlachos[1]
[1]Department of Chemical Engineering, University of Delaware, Newark, DE, USA
[2]U.S. Army Research Lab, Aberdeen Proving Ground, MD, USA

Abstract: The development of a high efficiency integrated thermoelectric/microcombustor device to generate power is described in this paper. An experimental evaluation of a prototype device was first analyzed using hydrogen as the fuel. In order to further improve the thermal efficiency of the device, an optimization study of the device configuration using a pseudo-3D energy balance model has been carried out. The model enabled the calculation of temperatures at each interface of the various elements that constitute the device and to determine the location of thermal losses from the device. It is shown that higher thermal efficiency can be obtained by stacking multiple thermoelectric elements in series as opposed to having just one thermoelectric element between the heat source and the heat sink. Furthermore, designs with thermoelectric elements stacked on both sides of the reactor were compared to designs with thermoelectric elements stacked on one side of the reactor with the other side of the reactor being thermally insulated. It was found that the single-sided design achieved a higher thermal efficiency while also utilizing less thermoelectric elements compared to the double-sided design, therefore providing a cost and size benefit. Experimental verification of these modeling results is also presented.

Keywords: Thermoelectric, Catalytic Microcombustor, Portable Power Generation

INTRODUCTION

Of the various efforts targeted towards utilizing hydrocarbon fuels for portable power generation [1], one approach gaining attention is the utilization of a catalytic micro-reactor to generate heat [2], which is then converted into electrical power using energy conversion modules, such as thermoelectric devices. A thermoelectric device operates on the principle of the Seebeck effect. This principle has led to the use of thermoelectric modules as energy scavengers in waste heat recovery systems. A considerable effort has been devoted to improve the efficiency of the heat source, the heat sink and the thermoelectric module itself. However, there has been no attempt at analyzing the configuration of the various elements that constitute the power device in order to improve efficiency. The objective of this paper is to analyze the arrangement of the source-thermoelectric-sink elements in order to optimize the performance of integrated devices that implement thermoelectric elements. The paper follows the following outline - experimental analysis of an integrated microcombustor / thermoelectric device is first presented. These results are followed by a modeling study to optimize the efficiency of source-thermoelectric-sink arrangements. The final section presents an experimental verification of the modeling predictions using a ceramic heater as the heat source.

EXPERIMENTAL INTEGRATED DEVICE

Device Design

A schematic of the prototype integrated device is shown in Fig. 1. The microcombustor consists of two square copper plates (shown in the inset of Fig. 2) of 30x30 mm and 3.2 mm thick. A three-legged serpentine channel was machined onto one plate, with each leg being approximately 22mm long, 6.25mm wide and 0.5mm deep. Two copper tubes, one at each end of the channel, were welded to the side of the plate to form the inlet and outlet ports.

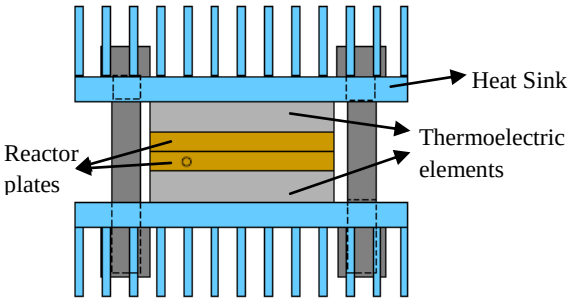

Figure 1: Schematic of integrated thermoelectric/ microcombustor device shown without any thermal insulation.

The fabrication of the catalytic inserts that were placed in the channel is detailed in [3]. The microcombustor was sandwiched between two thermoelectric modules (HZ-2, Hi-Z Technology, Inc.) with a heat-sink (Alpha LPD54-15B, Alpha Novatech) placed on the cold side of each thermoelectric module. It has been shown [4] that

the compressive load on a thermoelectric module plays a significant role in the power generated by the module. The device was held together using four bolts and a total load of approximately 186 lbs was applied using disc springs on each bolt. Aluminum nitride wafers (0.25 mm thick) were placed between each element of the device to prevent electrical shorting of the thermoelectric modules and each interface was coated with thermal grease (Hi-Z Technology, Inc.) to achieve good thermal contact. All the elements (except the heat-sinks) are wrapped with aero-gel insulation and aluminum tape to minimize radiation losses.

Device Operation and Experimental Results

The performance of the device was evaluated by flowing stoichiometric mixtures of H_2/air, with total flow rates ranging from 600 cc/min to 1000 cc/min, using flow controllers (MKS Instruments). Thermocouples were installed on the side wall of the microcombustor, on the inlet and outlet copper tubes and on the heat-sinks. Output power was measured by connecting a potentiometer in series with the thermoelectric module and measuring the load voltage and current as a function of load resistance to determine maximum power generated by the module. To prevent damage to the thermoelectric modules, the temperature of the microcombustor was limited to a maximum of 200˚C.

Figure 2 shows a plot of device efficiency, microcombustor temperature and heat-sink temperature as a function of input flow rate. Analysis of energy distribution reveals that the convective heat loss from the device surfaces (other than the heat sink) accounts for approximately 7% to 15% of total energy input which is a significant enhancement over previous designs [4]. However, the maximum efficiency of 0.57% obtained from this device did not offer any improvement over previous work [4]. In order to understand the reason for the low efficiency of the integrated device, the flow of energy through the device is analyzed using a pseudo-3D energy balance model presented next.

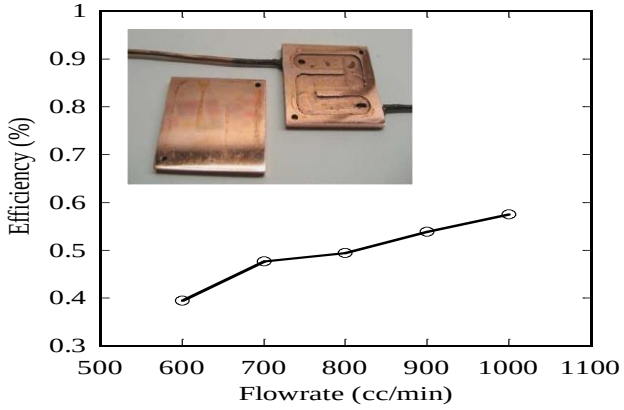

Figure 2: Efficiency of the integrated device vs. the total gas flow rate through the microcombustor. Inset shows a photograph of the serpentine channel microcombustor used.

ENERGY BALANCE MODEL

Applying symmetry, energy flow on only one side of the microcombustor is considered. Figure 3 shows the flow of energy between the various components of the system and also the losses from the system. The model is used to determine the effect of stacking thermoelectric modules in series and also to compare designs with thermoelectric elements stacked on both sides of the reactor to designs with thermoelectric elements stacked on one side of the reactor (with the other side of the reactor being thermally insulated). It is assumed that the microcombustor is of uniform temperature (T_R). The

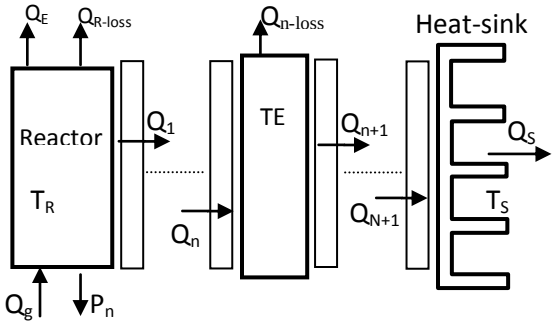

Figure 3: Schematic showing the flow of energy on one side of the integrated device.

amount of energy input to the system is the chemical energy of the fuel, which is designated as Q_g. For the purpose of calculating the convective heat losses, the insulation was divided into segments, with each segment having the same height as the component around which it was wrapped.

Heat loss from the thermoelectrics was assumed to occur at an average of the hot and cold side temperature of the thermoelectric module. Modeling of the entire system can be carried out by considering the energy balance around a single thermoelectric moule. The energy input (and output) into the thermoelectric can be derived by considering the Peltier effect, the Joule heating and heat conduction through the thermoelectric. On the hot side of the nth thermoelectric, one has

$$Q_n = S_n I_n T_n^H + \frac{k_t A_t}{L_t}(T_n^H - T_n^C) - \frac{I_n^2 R_T}{2} \quad (1)$$

Similarly on the cold side of the nth thermoelectric

$$Q_{n+1} = S_n I_n T_n^C + \frac{k_t A_t}{L_t}(T_n^H - T_n^C) + \frac{I_n^2 R_T}{2} \quad (2)$$

where, for the n[th] thermoelectric, I_n is the output current, Q_n is the heat input, S_n is the seebeck coefficient, k_t is the thermal conductivity, A_t is the contact area of the thermoelectric, L_t is the thickness of the thermoelectric, R_t is the internal resistance, and T_n^H and T_n^C are the hot and cold side temperatures of the thermoelectric. The output power of the n[th] thermoelectric is given by

$$P_n = Q_n - Q_{n+1} = I_n^2 R_L \quad (3)$$

where, R_L is the load resistance across which the power is measured. From the above equations, an expression for the output current can be obtained

$$I_n = S_n(T_n^H - T_n^C)/(R_T + R_L) \quad (4)$$

The heat loss from the reactor surface will depend on whether the device is double-stacked or single-stacked. A variable '*b*' is defined such that if the device is double-stacked then *b*=2 and if the device is single-stacked then *b*=1. The heat input to the first thermoelectric closest to the microcombustor is given by

$$Q_1 = \frac{1}{b}[Q_g - \dot{m}c_p(T_R - 298) - Q_{R-loss}] \quad (5)$$

where, $\dot{m}$ is the mass flow rate through the microcombustor, c_p is the specific heat capacity, and $Q_{R\text{-}loss}$ is the convective heat lost from the reactor hardware. The hot-side temperature of the first thermoelectric is then calculated

$$T_1^H = T_R - (L_c Q_1 / k_c A_{c-face}) \quad (6)$$

where, L_c, A_c and k_c are the thickness, contact area and thermal conductivity of the aluminum nitride wafer respectively. The solution is obtained by assuming a reactor temperature (T_R) and calculating T_1^H, which is then used subsequently to calculate the remaining temperatures. Assuming that the heat loss from the thermoelectric occurs at a temperature equal to $(T^H+T^C)/2$, the heat transfer from the cold side of the thermoelectric is given by

$$Q_{n+1} = Q_n - \left(\frac{1}{Zres_{TE}}\right)\left(\frac{T_n^H + T_n^C}{2} - T_{amb}\right) - \left(\frac{S_n(T_n^H - T_n^C)}{R_T + R_L}\right)^2 R_L \quad (7)$$

where, $Zres_{TE}$ is the thermal resistance of the insulation segment around each thermoelectric. Equations (2) and (7) can be solved to obtain T_n^C after which Q_{n+1} is calculated using eq. (7). The thermal conductivity of the wafer can then be used to calculate the hot-side temperature of the next thermoelectric similar to equation (6). These equations are repeated in a loop for the N thermoelectrics in the stack. The heat loss from the final (N) thermoelectric is equated to the heat loss from the heat sink given by

$$Q_{N+1} = \frac{1}{R_{sink}}(T_{N+1}^H - T_o) \quad (8)$$

where, R_{sink} is the manufacturer specified heat transfer resistance of the heat sink. The control temperature, T_o, is calculated form equation (10) and is checked against the value for the ambient temperature (T_{amb}). The solution is iterated until the value of the control temperature (T_o) at the end of the stack matches the ambient temperature. The efficiency of the system is given by

$$\eta_{sys} = \frac{P_s}{Q_g} \quad (9)$$

where P_S is the total output power of the device.

Modeling Results

Figure 4 shows the comparison of microcombustor temperature, heat-sink temperature and device efficiency between the model and experimental values of the integrated device. The temperature and efficiency curves show very good agreement between the model and the experimental

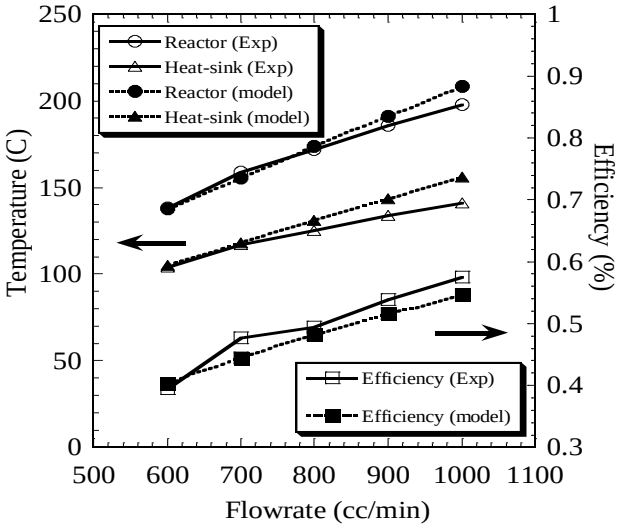

Figure 4: Comparison of the experimental and model values of reactor temperature, heatsink temperature and device efficiency.

values. The deviation between the curves at higher

flow rates is due to the incomplete conversion of the reactants in the experimental data which has not been considered in the model.

Having validated the model, Fig. 5 compares the total system efficiency for single-sided stacked and double-sided stacked device as a function of the total number of thermoelectrics for a stoichiometric inlet

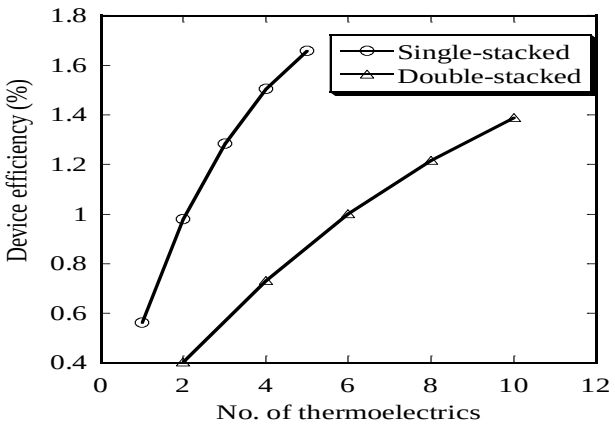

Figure 5: Device efficiency of single-sided stacked and double-sided stacked arrangements as a function of the total number of thermoelectric devices.

gas flow rate of 600cc/min. The single-stacked device clearly exhibits a much higher efficiency than the double-stacked device with the disparity increasing as more thermoelectrics are added to the device. In both cases, the system efficiency increases when thermoelectrics are stacked with the trend showing that adding more thermoelectrics will produce a nearly linear increase in system efficiency.

EXPERIMENTAL VALIDATION OF OPTIMIZATION RESULTS

In order to experimentally test the optimization results of the model, the microcombustor in Fig. 1 was replaced with a ceramic heater having similar dimensions as that of the microcombustor. Four configurations were tested using this setup – two double-sided and two single-sided arrangements. In the case of the single-sided configuration, one side of the microcombustor was covered with a 1 cm thick layer of aero-gel and, to provide a rigid support, a PTFE block was used in place of the heat-sink. In all four cases the input power was adjusted so that the heater reached a temperature of approximately 200°C. Figure 6 shows the system efficiency versus the total number of thermoelectrics used in each configuration. The results show that, for the same number of thermoelectric elements, a higher efficiency is obtained using a single-sided

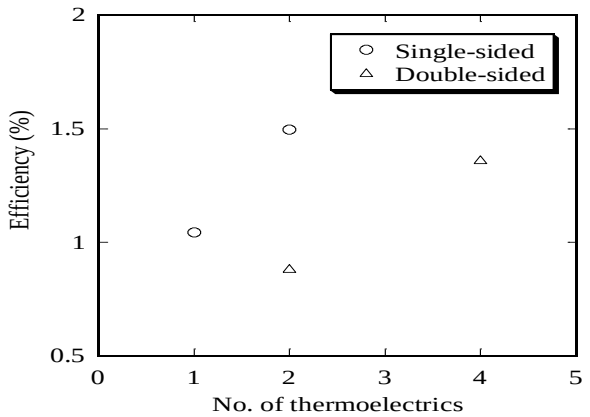

Figure 6: Experimental device (with ceramic heater) efficiency of single-sided stacked and double-sided stacked arrangements as a function of the total number of thermoelectric devices.

configuration compared to the double-sided design. Efficiency of the device can be further improved by stacking elements in series.

CONCLUSIONS

For devices that utilize thermoelectrics to scavenge heat to convert to electric power, our model predicts that an optimal design would be to stack thermoelectric modules on one side and insulating the other sides of the heat source. The model also shows that designs with thermoelectric elements stacked on one side of the reactor with the other side of the reactor being thermally insulated achieve a higher thermal efficiency while also utilizing less thermoelectric elements compared to the double-sided design, therefore providing a cost and size benefit. These results were also experimentally verified with the use of an electrical heater as the heat source.

REFERENCES

[1] Jacobson S.A. and Epstein A.H., *The Int. Symp. on Micro-Mech. Engg.,*Tsukuba, Japan,2003

[2] Karim A.M., Federici J.A. and Vlachos D.G., *Journal of Power Sources*, **179(1)**, 113-120.

[3] Norton D.G., Wetzel E.D. and Vlachos D.G., Ind. Eng. Chem. Res. **45** , 76–84

[4] Federici, J.A., Norton D.G., Wetzel E.D., and Vlachos D.G., *J. of Power Sources*, **161**(2) 1469-1478.